Ginsenoside compound K alleviates osteoarthritis by inhibiting NLRP3-mediated pyroptosis

YUGUO LI[1*], JIANG WU[2,3*] and NAIQIANG ZHUO[4]

[1]School of Clinical Medicine, Southwest Medical University, Luzhou, Sichuan 646000; [2]School of Clinical Medicine, Guizhou Medical University, Guiyang, Guizhou 550025; [3]Department of Orthopedic Surgery, Chinese People's Liberation Army General Hospital, Beijing 100853; [4]Department of Orthopedics, The Affiliated Hospital of Southwest Medical University, Luzhou, Sichuan 646000, P.R. China

Received November 8, 2022; Accepted April 28, 2023

DOI: 10.3892/etm.2023.12105

Abstract. Ginsenoside compound K (GCK) has been previously reported to be a potent antiarthritic and bone-protective agent. Therefore, the present study aimed to explore the potential effects of GCK on osteoarthritis and its regulatory effects on the pyroptosis of chondrocytes. Primary mouse chondrocytes (PMCs) were used for *in vitro* analysis. ELISA assays revealed that compared with the untreated cells, TNF-α induced a significant increase in IL-6, MMP13, A disintegrin and metalloproteinase with thrombospondin motifs 5 and MMP3 expression but induced a significant decrease in aggrecan and collagen II expression. By contrast, GCK reversed the aforementioned alterations in a dose-dependent manner. Experimental osteoarthritis was subsequently induced in mice through transection of the medial meniscotibial ligament and medial collateral ligament in the right knee [destabilization of the medial meniscus (DMM) mice]. GCK was found to reduce cartilage degradation *in vivo* in DMM mice, which was assessed using the Osteoarthritis Research Society International (OARSI) score, collagen II and MMP13 expression. Cartilage degradation is associated with higher OARSI score, decreased collagen II and increased MMP13 expression. In PMCs, TNF-α treatment stimulated an increase in the expression of NLR family pyrin domain containing 3 (NLRP3), Gasdermin D-N terminal (GSDMD-NT), cleaved caspase-1 and mature IL-1β, markers that indicate the occurrence of pyroptosis. However, GCK treatment suppressed the increase of the aforementioned proteins in a dose-dependent manner. Immunohistochemistry staining of the knee joint tissue sections from the DMM mice confirmed that GCK attenuated the NLRP3 and GSDMD-NT expression that was induced by DMM surgery. In conclusion, the present study revealed that GCK can reduce cartilage degradation in an osteoarthritis model by inhibiting the NLRP3-inflammasome activation and subsequent pyroptosis.

Correspondence to: Dr Naiqiang Zhuo, Department of Orthopedics, The Affiliated Hospital of Southwest Medical University, 25 Taiping Road, Jiangyang, Luzhou, Sichuan 646000, P.R. China
E-mail: qli86444@sina.com

*Contributed equally

Key words: ginsenoside compound K, osteoarthritis, pyroptosis, extracellular matrix, NLR family pyrin domain-containing 3

Introduction

In normal physiological conditions, chondrocytes respond to degradative inflammatory cascades by upregulating the biosynthesis of extracellular matrix (ECM) and secreting anti-inflammatory cytokines, such as IL-4, IL-10 and IL-13 (1). However, during the pathological development of osteoarthritis, the excessive generation and accumulation of inflammatory cytokines and MMPs interrupt the balance, which lead to cartilage degradation and chondrocyte cell death (1). Recent studies have indicated that pyroptosis, a lytic and inflammatory form of programmed cell death, is also involved in the development of osteoarthritis (2-4). The activation of caspase-1 induces the generation of proinflammatory cytokines, such as IL-1β and IL-18, resulting in pyroptosis (5).

Ginseng is a well-known herbal medicine in Asia. *Panax ginseng* is the most commonly used type of ginseng and has been applied to ameliorate rheumatoid arthritis and osteoarthritis in Asian countries (6). Ginsenosides are the major active compounds that can be found in ginseng (6). A number of ginsenosides have been reported to exert potent anti-inflammatory effects and are potential therapeutic agents for bone remodeling (7). In human osteoarthritis chondrocytes and a rat model of anterior cruciate ligament transection, Ginsenoside Rg1 reduced the expression of IL-1β-induced MMP13, cyclooxygenase-2 (COX-2) and prostaglandin E2, whilst also reversing the degradation of collagen II and aggrecan (8). Furthermore, ginsenoside Rb1 was previously demonstrated to alleviate monoiodoacetate-induced osteoarthritis by reducing cartilage degradation (9,10). Mechanistically, ginsenoside Rb1 was reported to suppress MMP13 expression by downregulating the Notch signaling pathway (11). Additionally, ginsenoside Rb1 can prevent chondrocyte apoptosis by

reducing the production of reactive oxygen species and activating the NF-κB signaling pathway (12).

Ginsenoside compound K (GCK) is a secondary ginsenoside that is bio-transformed from major ginsenosides, such as ginsenoside Rb1, Rb2 and Rc (13). Compared with their parental forms, GCK has higher bioavailability and increased water solubility (14,15). A previous study confirmed the potent antiarthritic and bone-protective effect of GCK (16). To facilitate the clinical utilization of GCK, it is necessary to elucidate its molecular mechanisms. The anti-inflammatory effects of GCK (17) and its parent forms (18) have been associated with their anti-pyroptotic properties. Ginsenoside Rb1 can reduce the pyroptosis of cardiomyocytes triggered by aconitine (19), whilst ginsenoside Rb2 can inhibit adipocyte pyroptosis and improve insulin resistance (20).

Therefore, the present study aimed to explore the potential effects of GCK on osteoarthritis and its regulatory effects on the pyroptosis of chondrocytes.

Materials and methods

Ethics statement. All animal-related experiments were approved by the Institutional Animal Care and Use Committee of Chinese People's Liberation Army General Hospital [approval no. SCXK(JING)2019-0010; Beijing, China]. In addition, it is confirmed that animals were anesthetized and sacrificed using acceptable methods and techniques.

Primary mouse chondrocytes (PMCs) culture. PMCs were prepared and cultured following the protocols described previously (21). Briefly, three 5-day-old neonatal C57BL/6 mice that had been euthanized with CO_2 inhalation (30% volume/min for at least 50 min) were purchased from SPEF (Beijing) Biotechnology Co., Ltd. Subsequently, the knee cartilage was isolated and digested using collagenase D solution at 0.5 mg/ml overnight at 37˚C (MilliporeSigma) to obtain PMCs. PMCs were cultured in DMEM/F12 (HyClone; Cytiva) supplemented with 10% fetal bovine serum (FBS; Gibco; Thermo Fisher Scientific, Inc.), 100 U/ml penicillin and 0.1 mg/ml streptomycin (Gibco; Thermo Fisher Scientific, Inc.) in a culture dish at a density of $8x10^3$ cells/cm^2 under standard conditions (37˚C, 5% CO_2). After achieving confluence by days 6-7 of culture, PMCs were harvested using 0.25% Trypsin-EDTA (Gibco; Thermo Fisher Scientific, Inc.) and passaged. Passage two cells were used for all experiments.

Cell viability assay and ELISA. PMCs were seeded into 96-well plates (5,000 cells/well) and then subjected to the selective treatments in sequential order: i) GCK (Chengdu Zhibiao Pure Biotechnology Co., Ltd.) pre-treatment (10 or 50 μM) for 24 h; ii) TNF-α (20 ng/ml; Beyotime Institute of Biotechnology) treatment for 12 h; and iii) GCK post-treatment (10 or 50 μM) for 12 h. Cells that received DMSO served as a negative control. Three sets of experiment groups were designed: Treatment i alone; treatment ii alone; and treatment i, ii and iii in combination. To check the influence of GCK on the viability of PMCs, cells in 96-well plates (5,000 cells/well) were cultured in the presence of different concentrations of GCK (0, 10, 20, 50, 100 and 150 μM) for 48 h. The cell viability of PMCs was then measured using a Cell Counting Kit-8 (CCK-8) assay (Dojindo Molecular Technologies, Inc.) following the manufacturer's instructions. In brief, 10 μl of CCK-8 solution was added to each well and incubated for 2 h. The absorbance at 450 nm was measured using an ELISA reader (Hangzhou Lianke Biotechnology Co., Ltd.).

Commercial ELISA kits were used to determine the concentration of IL-6 (cat. no. PI326; Beyotime Institute of Biotechnology), MMP13 (cat. no. YB-MMP13-Mu; Shanghai Yubo Biotechnology Co., Ltd.), A Disintegrin and Metalloproteinase with Thrombospondin Motifs 5 (ADAMTS5) (cat. no. LS-F32114; LifeSpan BioSciences, Inc.), MMP3 (cat. no. YB-MMP3-Mu; Shanghai Yubo Biotechnology Co., Ltd.), aggrecan (cat. no. YB-AGC-Mu; Shanghai Yubo Biotechnology Co., Ltd.) and collagen II (cat. no. YB-PIINP-Mu; Shanghai Yubo Biotechnology Co., Ltd.) in the culture supernatants after the aforementioned treatments, following the manufacturer's protocols.

Immunofluorescence staining. PMCs ($1x10^5$) were cultured on glass coverslips in 24-well plates and then, in sequential order, were treated as follows: i) Pre-treated with GCK (50 μM) for 24 h; ii) treated with TNF-α (20 ng/ml) for 12 h; and iii) post-treated with GCK (50 μM) for another 12 h. Cells that received DMSO treatment served as a negative control. Three sets of experiment groups were designed: Treatment i alone; treatment ii alone; and treatment i, ii and iii in combination. Following treatment, the cells were fixed in 4% paraformaldehyde for 15 min at room temperature, treated with 0.1% Triton X-100 and blocked using 3% bovine serum albumin (Gibco; Thermo Fisher Scientific, Inc.) for 1 h at room temperature. The coverslips were then incubated with anti-MMP13 (1:200; cat. no. 18165-1-AP; Wuhan Sanying Biotechnology) or anti-collagen II (1:200; cat. no. ab34712; Abcam) at 4˚C overnight. After washing three times with PBS (5 min/time) at room temperature, the coverslips were incubated with a secondary antibody (1:1,000; CoraLite488-conjugated anti-rabbit; cat. no. SA00013-2; Wuhan Sanying Biotechnology) at room temperature for 2 h. The nucleus was stained using DAPI (300 nM; Thermo Fisher Scientific, Inc.) for 5 min at room temperature in the dark.

For TUNEL staining, the fixation and Triton X-100 treatments were the same as aforementioned. A One Step TUNEL Apoptosis Assay Kit (cat. no. C1086, Beyotime Institute of Biotechnology) was used. TUNEL detection solution (50 μl) was added to the sample and incubated at 37˚C in the dark for 60 min. After washing two times with PBS (5 min/time) at room temperature, the fluorescence was detected. TUNEL-positive cells in five random views were quantified by manual counting. Fluorescent images were captured using a confocal microscope under x20 or x40 magnification (Leica Microsystems GmbH).

Animal studies. Pathogen-free WT C57BL/6J male mice (n=24; 2-month-old; body weight, 25-30 g) were obtained from SPEF (Beijing) Biotechnology Co., Ltd. The mice were housed in a temperature-controlled environment (temperature, 25±2˚C; relative humidity, 45-60%) with a 12-h light/dark cycle and received food and water *ad libitum*.

Before the experimental surgery, mice were anesthetized with 250 mg/kg intraperitoneal tribromoethanol (Avertin; Sigma-Aldrich; Merck KGaA). To prepare the 100% Avertin

stock solution, 10 g tribromoethanol was added into a centrifuge tube with 10 ml tertiary amyl alcohol. The tube was then shaken in hand until the tribromoethanol was completely dissolved. The solution was then filtered using a 0.22-μm filter membrane. A working solution of 2.5% Avertin was prepared by diluting the 100% Avertin stock solution to 2.5% (1:40) with 0.9% NaCl. The working solution was stored at 4˚C in the dark and used within 2 weeks.

Experimental osteoarthritis was induced in the mice through transection of the medial meniscotibial ligament and medial collateral ligament in the right knee [destabilization of the medial meniscus (DMM) mice]. The left knees not subjected to surgery in the DMM alone group and was used as the control (sham) for both DMM and DMM + GCK groups. According to previous studies, 40 mg/kg GCK was sufficient to exert anti-inflammatory effects in both rat and mouse models of induced arthritis (22,23). The day after the surgery, the mice were fed for 8 weeks either with a control diet (normal diet) or with diets supplemented with GCK (40 mg/kg) (biological replicates, n=12 per group). Mice were euthanized with CO_2 inhalation (30% volume/min for at least 10 min) after 8 weeks of surgery. Euthanasia using CO_2 was conducted following the AVMA Guidelines for the Euthanasia of Animals (2020 edition). The mice were left in the CO_2 environment until the cessation of breathing and heartbeat, when fully dilated pupils were observed. Knee joints were then collected for histological analysis.

Immunohistochemistry (IHC), Safranin O-Fast Green and H&E staining. IHC, Safranin O-Fast Green and H&E staining were conducted in paraffin-embedded tissues using the BOND-III Automated IHC Stainer (Leica Microsystems GmbH). Knee joints were fixed in neutral buffered formalin at a concentration of 10%, at room temperature for 16 h. Dehydration was performed in graded alcohols (70, 95 and 100% ethanol). Next, the tissues were cleared in a clearing agent (xylene substitute) to remove alcohol and prepare them for infiltration with paraffin wax. The tissues were then infiltrated with liquid paraffin wax at 56-60˚C for 6 h until they became fully embedded. After that, the tissues were transferred into fresh liquid paraffin wax and allowed to cool and solidify. Sections (5 μm) were set in the Stainer. Antigens were retrieved by heating the tissue sections in a BOND Epitope Retrieval ER2 Solution contained in the BOND IHC Polymer Detection Kit (cat. no. DS9800) for 20 min at 100˚C. Tissues sections were then subjected to peroxide blocking using the hydrogen peroxide included in the BOND IHC Polymer Detection Kit (cat. no. DS9800) for 5 min. The following primary antibodies were used: Anti-collagen II (1:600; cat. no. 28459-1-AP; Wuhan Sanying Biotechnology), anti-MMP13 (1:250; cat. no. 18165-1-AP; Wuhan Sanying Biotechnology), anti-NLR family pyrin domain-containing 3 (anti-NLRP3; 1:200; cat. no. 19771-1-AP; Wuhan Sanying Biotechnology) and anti-Gasdermin D-N terminal (anti-GSDMD-NT; 1:800; cat. no. 36425; Cell Signaling Technology, Inc.). The tissue sections were incubated with the diluted primary antibodies for 30 min at room temperature and then washed three times with BOND Wash Solution (2 min/time). Next, the sections were incubated with an HRP-conjugated secondary antibody (1:2,000) contained in the BOND IHC Polymer Detection Kit (cat. no. DS9800) for 10 min at room temperature. Chromogenic detection was conducted by incubating tissue sections with DAB for 10 min. Counterstaining was conducted by incubating the tissue sections with hematoxylin for 5 min at room temperature. DAB and hematoxylin were contained in the BOND IHC Polymer Detection Kit (cat. no. DS9800). The IHC staining was quantified using a scoring system described previously (24). The percentage of positive cells was scored as follows: i) Score of 1, ≤24%; ii) score of 2, 25-50%; iii) score of 3, 51-75%; and iv) score of 4, ≥76%. The intensity of IHC staining was scored as follows: i) Score of 0, negative; ii) score of 1, weak; iii) score of 2, moderate; and (iv) score of 3, strong. The total score was calculated as follows: Total score = positive percentage score x intensity score.

For Safranin O-Fast Green and H&E staining, the Safranin O-Fast Green staining kit (cat. no. PH1852; Phygene) and the H&E staining kit (cat. no. PH0516; Phygene) were loaded into BOND-III Automated IHC Stainer. For Safranin O-Fast Green staining, after deparaffinization and rehydration as aforementioned, the tissue sections were incubated with Safranin O solution for 10 min at the room temperature. Next, the sections were washed with 70% ethanol for 30 sec. The sections were then incubated with Fast Green solution for 5 min. After the staining, the sections were washed with graded alcohols (80, 95 and 100%) for 30 sec each. Finally, the sections were washed with xylene (2X) for 1 min. For H&E saining, after deparaffinization and rehydration, the tissue sections were incubated hematoxylin solution for 10 min at the room temperature and then washed with bluing reagent for 5 min. Next, the sections were incubated with eosin solution for 5 min. Washing with graded alcohols and with xylene was as aforementioned. The staining images were captured using a DM4000 B LED microscope (Leica Microsystems, Inc.) at x20 or x40 magnification.

Western blotting. Conventional western blotting was performed as previously described (25). Briefly, total proteins were extracted from the PMCs using RIPA lysis buffer (Beyotime Institute of Biotechnology) and protein concentration was determined using a BCA kit (cat. no. P0012; Beyotime Institute of Biotechnology). The proteins (25 μg/lane) were separated on 10% gels using SDS-PAGE, transferred onto nitrocellulose membranes, blocked using 5% BSA (Gibco; Thermo Fisher Scientific, Inc.) in TBST (0.1% Tween-20) at 37˚C for 30 min and then incubated with primary antibodies at 4˚C overnight. The following antibodies were used: Anti-NLRP3 (1:1,000; cat. no. 19771-1-AP; Wuhan Sanying Biotechnology), anti-GSDMD-NT (1:1,000; cat. no. 36425; Cell Signaling Technology, Inc.), anti-cleaved caspase-1 (1:1,000; cat. no. 89332; Cell Signaling Technology, Inc.), anti-mature IL-1β (1:1,000; cat. no. 83186; Cell Signaling Technology, Inc.) and anti-β-actin (1:2,000; cat. no. 20536-1-AP; Wuhan Sanying Biotechnology). The membranes were washed with 1X TBST three times (5 min/time) and incubated with HRP-conjugated secondary antibodies (1:5,000; cat. no. SA00001-2; Wuhan Sanying Biotechnology) at room temperature for 1 h. The protein bands were visualized using an enhanced chemiluminescence kit (BeyoECL Star; Beyotime Institute of Biotechnology) and ChemiScope 6200T imager (Clinx Science Instruments Co., Ltd.). The intensities of protein bands were quantitated using ImageJ (v1.5.4; National Institutes of Health) based on three biological repeats.

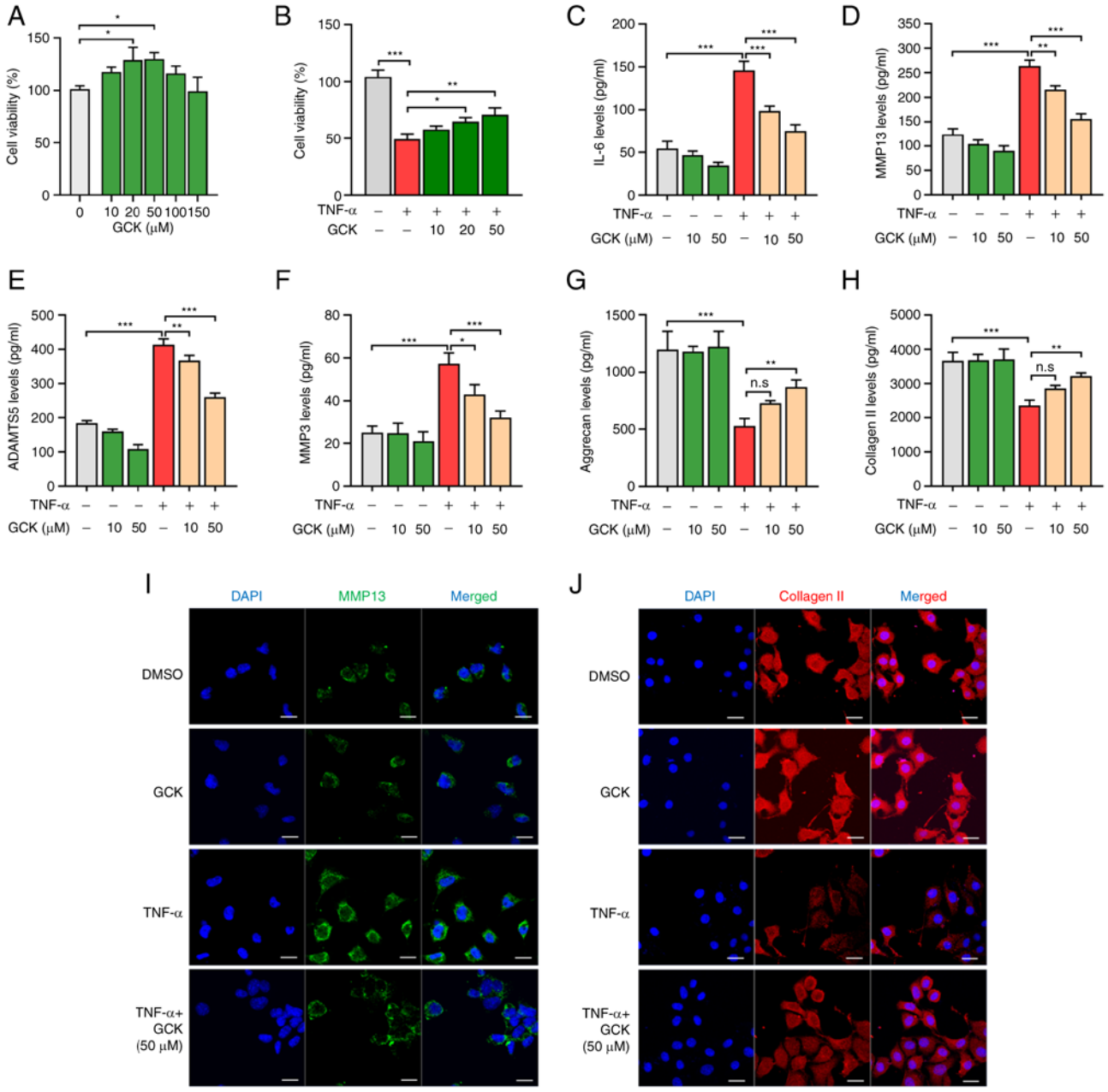

Figure 1. GCK reduces TNF-α-induced imbalance of extracellular matrix homeostasis in chondrocytes *in vitro*. (A and B) Cell viability of normal primary mouse chondrocytes after treatment with different concentrations of GCK (A) alone or (B) in combination with TNF-α treatment (20 ng/ml) for 48 h. Effects of TNF-α and GCK on (C) IL-6, (D) MMP13, (E) ADAMTS5, (F) MMP3, (G) aggrecan and (H) Collagen II production in chondrocytes after the indicated treatments. The protein concentrations were determined using ELISA (n=3). Immunofluorescence staining of (I) MMP13 (green) and (J) collagen II and the nucleus (DAPI; blue) in chondrocytes following the indicated treatments. The data are presented as the mean ± SD (n=3). Scale bar, 20 μm. *P<0.05, **P<0.01 and ***P<0.001. GCK, ginsenoside compound K; ADAMTS5, A Disintegrin and Metalloproteinase with Thrombospondin Motifs 5; Col II, collagen II; n.s, not significant.

Statistical analysis. Data are presented as the mean ± SD. Statistical analysis was conducted using GraphPad Prism 8.10 (GraphPad Software; Dotmatics). The Wilcoxon's signed-rank test was performed for Sham vs. DMM comparisons due to the paired nature of these two groups, whilst the Wilcoxon's rank-sum test was performed for DMM vs. DMM + GCK comparisons due to the unpaired nature of these two groups. Bonferroni's correction was conducted on all P-values yielded by these two aforementioned tests. Since two tests were performed within each group, P<0.025 was considered to indicate a statistically significant difference in these two cases. Either Kruskal-Wallis test followed by Dunn's test (staining scores) or one-way ANOVA followed by Tukey's post hoc test (numerical data) was used for the rest of the multiple comparisons in Figs. 1 and 3. P<0.05 was considered to indicate a statistically significant difference.

Results

GCK reduces the TNF-α-induced imbalance of ECM homeostasis in chondrocytes in vitro. To check the influence of GCK on the viability of PMCs, cells were cultured in the

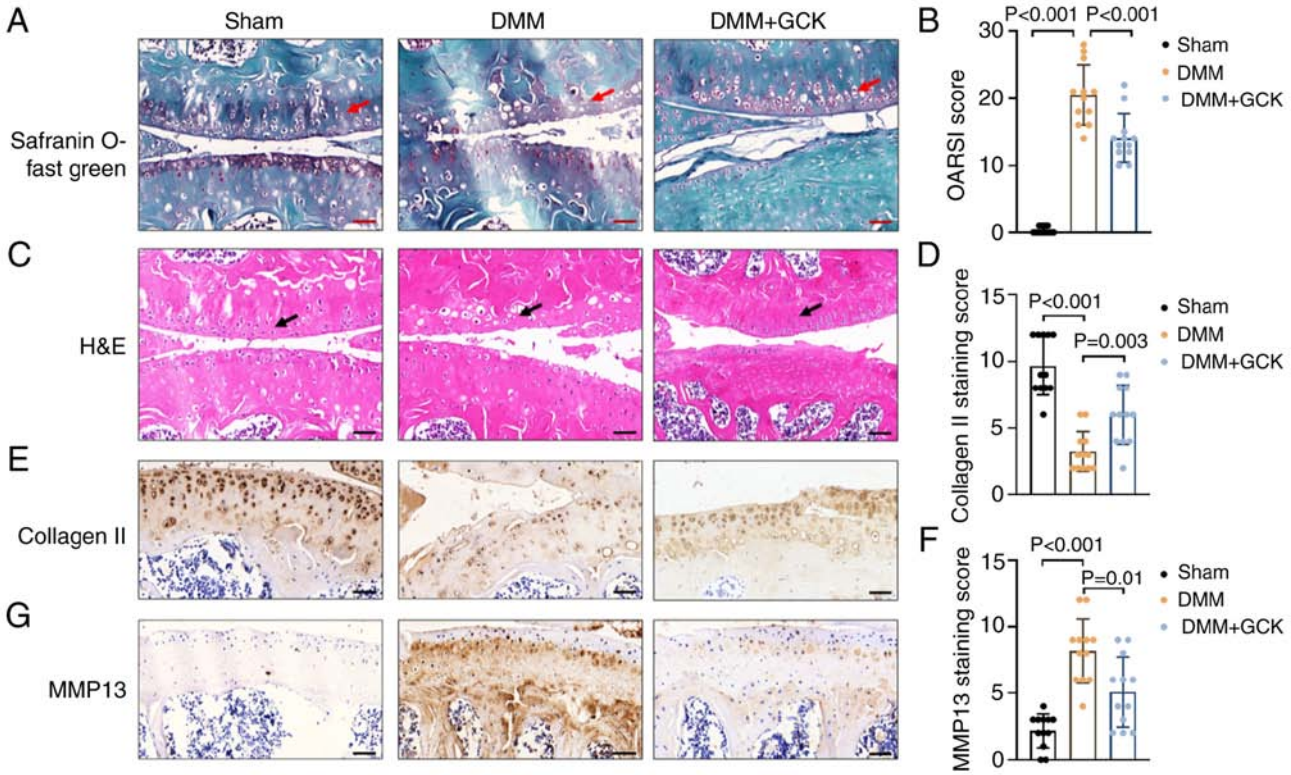

Figure 2. GCK reduces cartilage degradation *in vivo* in a surgically-induced model of osteoarthritis. Representative (A) Safranin O-Fast Green staining, (C) H&E staining (red and black arrows indicate the cartilage superficial zone), immunohistochemistry staining of (E) collagen II and (G) MMP13 of the cartilage from different groups at 8 weeks post-surgery. Scale bars, 50 μm. (B) The OARSI histological scores of the different treatment groups. Immunohistochemical quantification of (D) collagen II and (F) MMP13 expression. All data are presented as the mean ± SD (n=3). Sham represents the left knee tissues in the DMM-alone group, which did not undergo surgery. The sham and DMM tissues were from the same mouse. GCK, ginsenoside compound K; OARSI, Osteoarthritis Research Society International; DMM, destabilization of the medial meniscus.

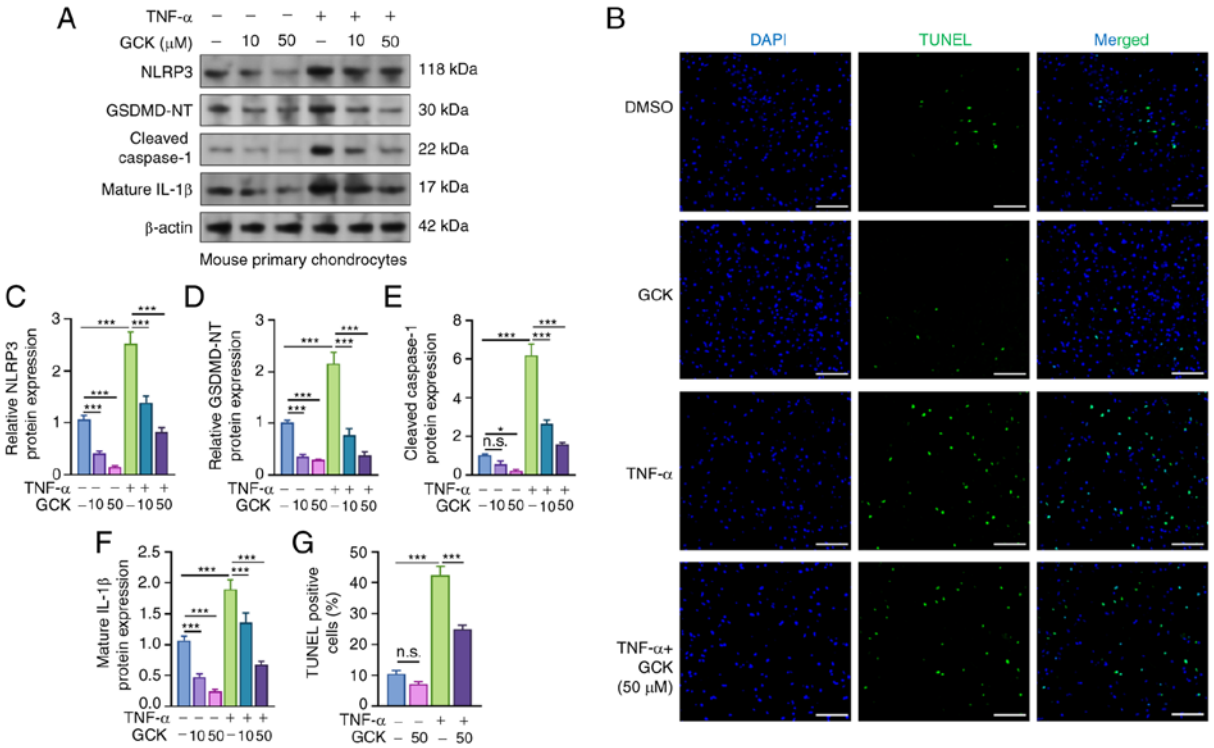

Figure 3. GCK suppresses osteoarthritis-associated NLRP3 inflammasome activation and pyroptosis. (A) Western blotting was conducted to measure the expression levels of (C) NLRP3, (D) GSDMD-NT, (E) cleaved caspase-1 and (F) mature IL-1β in the primary mouse chondrocytes treated as indicated. (G) Quantitation and (B) representative images of TUNEL positive PMCs treated as indicated. Scale bars, 100 μm. All data are presented as the mean ± SD (n=3). *P<0.05 and ***P<0.001. GCK, ginsenoside compound K; NLRP3, NLR family pyrin domain-containing 3; GSDMD-NT, Gasdermin D-N terminal; n.s, not significant.

presence of different concentrations of GCK (0, 10, 20, 50, 100 and 150 μM) for 48 h. CCK-8 assay results revealed that GCK conferred no cytotoxicity towards PMCs, even at the concentration of 150 μM (Fig. 1A). Furthermore, concentrations of 20 and 50 μM GCK significantly increased cell viability compared with that in the control cells (Fig. 1A). A total of 10 and 50 GCK μM were used in the following studies to assess whether GCK had dose-dependent effects on PMCs.

In addition, the viability of PMCs was found to be significantly reduced by TNF-α treatment. However, co-treatment with GCK (20 and 50 μM) significantly restored their cell viability (Fig. 1B). To assess the influence of GCK on TNF-α-induced inflammation and ECM dysregulation, the secretion of ECM regulatory factors were measured using ELISA. The results indicated that TNF-α induced a significant increase in IL-6, MMP13, ADAMTS5 and MMP3 levels (Fig. 1C-F), whilst significantly decreasing aggrecan and collagen II levels (Fig. 1G and H). GCK appeared to have reversed these alterations in a dose-dependent manner (Fig. 1C-H). Immunofluorescence staining also revealed that GCK partially suppressed the MMP13 expression that was induced by TNF-α whilst rescuing the collagen II expression that was reduced by TNF-α in PMCs (Fig. 1I and J).

GCK reduces cartilage degradation in vivo in a surgically-induced model of osteoarthritis. To explore the potential effects of GCK on osteoarthritis *in vivo*, an osteoarthritis model was established in mice by DMM surgery, without significant adverse effects among the animals, such as significant loss of body weight and consistent bleeding. Knee joints were collected, paraffin-embedded, sectioned and stained. Safranin O-Fast Green and H&E staining revealed that DMM surgery resulted in cartilage erosion in the femur and tibia, loss of the superficial zone and reduced uncalcified cartilage (red and black arrows; .. 2A and C). However, these pathological changes were mitigated by GCK supplementation (Fig. 2A and C).

To quantify the aforementioned changes, the sections were scored using the Osteoarthritis Research Society International (OARSI) semi-quantitative grading system, which assesses the lesion severity and the affected area in both the femur and tibia (26). The DMM group had a significantly increased OARSI score compared with that in the sham group (Fig. 2B). By contrast, the DMM mice treated with GCK had a significantly lower OARSI score compared with that in the DMM-only group (Fig. 2B). Protein expression was then assessed using immunohistochemistry. The mice treated with GCK exhibited significantly increased collagen II (Fig. 2E and D) and significantly decreased MMP13 expression (Fig. 2G and F) compared with that in the DMM-only group.

GCK suppresses osteoarthritis-associated NLRP3 inflammasome activation and pyroptosis. In PMCs, TNF-α treatment stimulated a significant increase in the levels of NLRP3, GSDMD-NT, cleaved caspase-1 and mature IL-1β, the markers indicating the occurrence of pyroptosis (5) (Fig. 3A and C-F). However, GCK treatment suppressed the increase of these proteins in a dose-dependent manner (Fig. 3A and C-F). TUNEL assay was then used to examine the extent of cell death of PMCs. The TNF-α treatment group had a significantly higher level of TUNEL-positive cells compared with that in the DMSO group (Fig. 3B and G). However, GCK treatment decreased the percentage of TUNEL-positive PMCs induced by TNF-α (Fig. 3B and G).

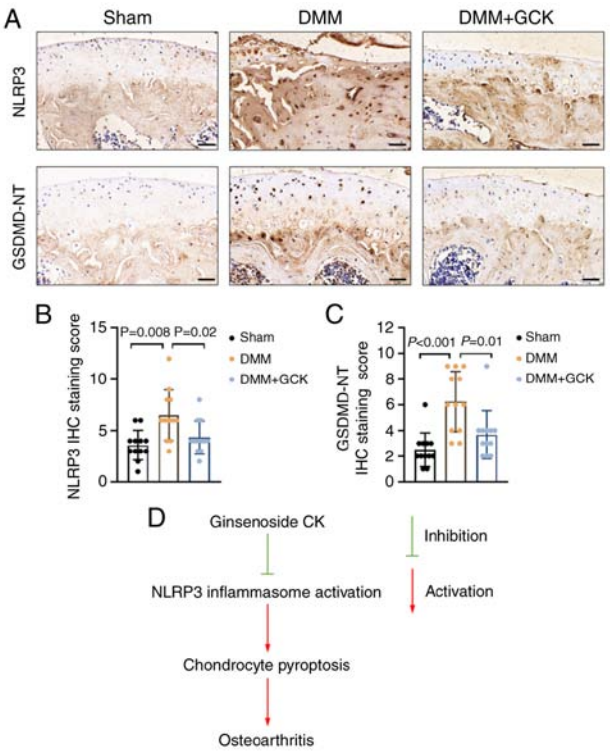

Figure 4. GCK suppresses osteoarthritis-associated pyroptosis *in vivo*. (A) Representative images of NLRP3 and GSDMD-NT in the three groups treated as indicated. Scale bars, 50 μm. Quantification scores of the immunohistochemistry analysis of (B) NLRP3 and (C) GSDMD-NT in the three groups treated as indicated. All data are presented as the mean ± SD (n=3). Sham represents the left knee tissues in the DMM-alone group, which did not undergo surgery. The sham and DMM tissues were from the same mouse. (D) A schematic diagram demonstrating the possible mechanisms of the ameliorative effects of GCK on osteoarthritis by inhibiting NLRP3-mediated pyroptosis. GCK, ginsenoside compound K; NLRP3, NLR family pyrin domain containing 3; GSDMD-NT, Gasdermin D-N terminal; DMM, destabilization of the medial meniscus; IHC, immunohistochemistry.

GCK suppresses osteoarthritis-associated pyroptosis in vivo. IHC analysis of the knee joint tissue sections from DMM mice with or without GCK treatment confirmed that NLRP3 and GSDMD-NT expression was significantly increased in the cartilage of the DMM mice compared with that in the sham control group (Fig. 4A-C). Compared with that in the DMM mice without GCK treatment, the DMM mice that received GCK treatment exhibited significantly reduced NLRP3 and GSDMD-NT expression (Fig. 4A-C).

Discussion

During the pathological development of osteoarthritis, the expression of inflammatory and catabolic factors is upregulated. Among these factors, IL-1β and TNF-α serve critical roles and can induce the expression of cartilage-degrading enzymes, such as MMP1, MMP3, MMP13, ADAMTS4 and ADAMTS5 (2,27). These factors can all contribute to the

degradation of aggrecans and type II collagen, leading to cartilage matrix damage (2). Furthermore, IL-1β and TNF-α can trigger inflammatory-associated chondrocyte cell death (2,27).

Pyroptosis has recently been characterized as an important component in osteoarthritis (28). Although it remains unclear whether pyroptosis serves as a cause or the result of cartilage degeneration, osteoarthritis-related risk factors, such as cholesterol, oxidized low-density lipoprotein and lipopolysaccharide, have been reported to initiate pyroptosis (29,30). Osteoarthritis-related risk factors mainly trigger chondrocyte pyroptosis through the NLRP3 inflammasome pathway to cause the upregulation of IL-1β and TNF-α (31,32). Therefore, the initiation of chondrocyte pyroptosis can disrupt the balance between the anabolism and catabolism of the chondrocyte ECM, resulting in ECM degradation (28). Inhibiting chondrocyte pyroptosis may prove to be a viable strategy to slow the progression of osteoarthritis (3,28).

The anti-inflammatory properties of GCK have been characterized in previous studies (14,16,33). GCK has been found to reduce the synthesis of proinflammatory cytokines IL-6, IL-1β, TNF-α, COX-2 and inducible nitric oxide synthase (14). Furthermore, GCK has been observed to exert anti-inflammatory and bone-protective effects in rheumatoid arthritis by inhibiting the production of MMP1 and MMP3 whilst suppressing the JNK and ERK pathways (16). GCK can also inhibit TNF receptor 2 expression to weaken TNF-α downstream signaling (16). In addition, GCK has been reported to promote the osteogenic differentiation of rat bone marrow mesenchymal stem cells by activating the Wnt/β-catenin signaling pathway (34). In the present study, it was demonstrated that GCK could alleviate the TNF-α-induced imbalance of ECM homeostasis in PMCs *in vitro*, in addition to reducing cartilage degradation *in vivo* in a surgery-induced model of osteoarthritis. These results support the presence of chondrocyte protective effects of GCK.

Although the parental forms of GCK have demonstrated anti-pyroptotic effects in various human cells, such as human induced pluripotent stem cell-derived cardiomyocytes and adipocytes (19,20), whether GCK can exert anti-pyroptotic effects in chondrocytes remain unclear. In high-fat diet/streptozotocin-induced diabetic mice, GCK has been documented to protect against diabetic nephropathy by suppressing NLRP3 inflammasome activation and the NF-κB/p38 signaling pathway (18). Using PMCs, the present study demonstrated that GCK suppressed osteoarthritis-associated NLRP3 inflammasome activation and pyroptosis. IHC staining of the knee joint tissue sections from DMM mice found that GCK attenuated the NLRP3 and GSDMD-NT expression that was induced by the DMM surgery. These findings suggest that GCK can alleviate osteoarthritis by inhibiting NLRP3-mediated pyroptosis in chondrocytes (Fig. 4D).

The present study has a number of limitations. Due to the absence of detection devices, whether GCK could alleviate the severe joint pain associated with osteoarthritis was not assessed. In addition, GCK as a natural product may have a series of docking proteins, which was not explored in the present study. Future studies are needed to resolve these issues.

In conclusion, the present study revealed that GCK could reduce cartilage degradation in a mouse model of osteoarthritis by inhibiting NLRP3-inflammasome activation and subsequent pyroptosis.

Acknowledgements

Not applicable.

Funding

The present study was funded by the Department of Orthopedics (The Affiliated Hospital of Southwest Medical University, China).

Availability of data and materials

The datasets used and/or analyzed during the current study are available from the corresponding author on reasonable request.

Authors' contributions

YL was involved in study conceptualization, data curation and formal analysis, investigation, developing the methodology, providing resources and software analysis. JW was involved in developing the methodology, providing resources, software analysis, data validation and visualization. NZ performed the conceptualization of the study, project administration, supervision, data validation and writing of the manuscript. YL and JW confirm the authenticity of all the raw data. All authors have read and approved the final manuscript.

Ethics approval and consent to participate

All animal-related experiments were approved by the Institutional Animal Care and Use Committee of Chinese People's Liberation Army General Hospital [Beijing, China; approval no. SCXK(JING)2019-0010].

Patient consent for publication

Not applicable.

Competing interests

The authors declare that they have no competing interests.

References

1. Coryell PR, Diekman BO and Loeser RF: Mechanisms and therapeutic implications of cellular senescence in osteoarthritis. Nat Rev Rheumatol 17: 47-57, 2021.
2. An S, Hu H, Li Y and Hu Y: Pyroptosis plays a role in osteoarthritis. Aging Dis 11: 1146-1157, 2020.
3. Yang J, Hu S, Bian Y, Yao J, Wang D, Liu X, Guo Z, Zhang S and Peng L: Targeting cell death: Pyroptosis, ferroptosis, apoptosis and necroptosis in osteoarthritis. Front Cell Dev Biol 9: 789948, 2022.
4. Wu Y, Zhang J, Yu S, Li Y, Zhu J, Zhang K and Zhang R: Cell pyroptosis in health and inflammatory diseases. Cell Death Discov 8: 191, 2022.
5. Miao EA, Leaf IA, Treuting PM, Mao DP, Dors M, Sarkar A, Warren SE, Wewers MD and Aderem A: Caspase-1-induced pyroptosis is an innate immune effector mechanism against intracellular bacteria. Nat Immunol 11: 1136-1142, 2010.
6. Yi YS: Ameliorative effects of ginseng and ginsenosides on rheumatic diseases. J Ginseng Res 43: 335-341, 2019.

7. Yang N, Liu D, Zhang X, Li J, Wang M, Xu T and Liu Z: Effects of ginsenosides on bone remodelling for novel drug applications: A review. Chin Med 15: 42, 2020.
8. Cheng W, Jing J, Wang Z, Wu D and Huang Y: Chondroprotective effects of ginsenoside Rg1 in human osteoarthritis chondrocytes and a rat model of anterior cruciate ligament transection. Nutrients 9: 263, 2017.
9. Aravinthan A, Hossain MA, Kim B, Kang CW, Kim NS, Hwang KC and Kim JH: Ginsenoside Rb1 inhibits monoiodoacetate-induced osteoarthritis in postmenopausal rats through prevention of cartilage degradation. J Ginseng Res 45: 287-294, 2021.
10. Luan J, Che G, Man G and Xiao F: Ginsenoside Rb1 from Panax ginseng attenuates monoiodoacetate-induced osteoarthritis by inhibiting miR-21-5p/FGF18-mediated inflammation. J Food Biochem 46: e14340, 2022.
11. Wang W, Zeng L, Wang ZM, Zhang S, Rong XF and Li RH: Ginsenoside Rb1 inhibits matrix metalloproteinase 13 through down-regulating Notch signaling pathway in osteoarthritis. Exp Biol Med (Maywood) 240: 1614-1621, 2015.
12. Hossain MA, Alam MJ, Kim B, Kang CW and Kim JH: Ginsenoside-Rb1 prevents bone cartilage destruction through down-regulation of p-Akt, p-P38, and p-P65 signaling in rabbit. Phytomedicine 100: 154039, 2022.
13. Zhang R, Huang XM, Yan HJ, Liu XY, Zhou Q, Luo ZY, Tan XN and Zhang BL: Highly selective production of compound K from Ginsenoside Rd by hydrolyzing glucose at C-3 glycoside using beta-Glucosidase of Bifidobacterium breve ATCC 15700. J Microbiol Biotechnol 29: 410-418, 2019.
14. Sharma A and Lee HJ: Ginsenoside compound K: Insights into recent studies on pharmacokinetics and health-promoting activities. Biomolecules 10: 1028, 2020.
15. Baik IH, Kim KH and Lee KA: Antioxidant, anti-inflammatory and antithrombotic effects of ginsenoside compound K enriched extract derived from ginseng sprouts. Molecules 26: 4102, 2021.
16. Tang M, Xie X, Yang Y and Li F: Ginsenoside compound K-a potential drug for rheumatoid arthritis. Pharmacol Res 166: 105498, 2021.
17. Song W, Wei L, Du Y, Wang Y and Jiang S: Protective effect of ginsenoside metabolite compound K against diabetic nephropathy by inhibiting NLRP3 inflammasome activation and NF-κB/p38 signaling pathway in high-fat diet/streptozotocin-induced diabetic mice. Int Immunopharmacol 63: 227-238, 2018.
18. Yi YS: Roles of ginsenosides in inflammasome activation. J Ginseng Res 43: 172-178, 2019.
19. Wang M, Wang R, Sun H, Sun G and Sun X: Ginsenoside Rb1 ameliorates cardiotoxicity triggered by aconitine via inhibiting calcium overload and pyroptosis. Phytomedicine 83: 153468, 2021.
20. Lin Y, Hu Y, Hu X, Yang L, Chen X, Li Q and Gu X: Ginsenoside Rb2 improves insulin resistance by inhibiting adipocyte pyroptosis. Adipocyte 9: 302-312, 2020.
21. Gosset M, Berenbaum F, Thirion S and Jacques C: Primary culture and phenotyping of murine chondrocytes. Nat Protoc 3: 1253-1260, 2008.
22. Chen J, Wang Q, Wu H, Liu K, Wu Y, Chang Y and Wei W: The ginsenoside metabolite compound K exerts its anti-inflammatory activity by downregulating memory B cell in adjuvant-induced arthritis. Pharm Biol 54: 1280-1288, 2016.
23. Liu KK, Wang QT, Yang SM, Chen JY, Wu HX and Wei W: Ginsenoside compound K suppresses the abnormal activation of T lymphocytes in mice with collagen-induced arthritis. Acta Pharmacol Sin 35: 599-612, 2014.
24. Wu CY, Li L, Chen SL, Yang X, Zhang CZ and Cao Y: A Zic2/Runx2/NOLC1 signaling axis mediates tumor growth and metastasis in clear cell renal cell carcinoma. Cell Death Dis 12: 319, 2021.
25. Li Y, Chen S, Zhang X and Zhuo N: U2 small nuclear RNA auxiliary factor 2, transcriptionally activated by the transcription factor Dp-1/E2F transcription factor 1 complex, enhances the growth and aerobic glycolysis of leiomyosarcoma cells. Bioengineered 13: 10200-10212, 2022.
26. Moskowitz RW: Osteoarthritis cartilage histopathology: Grading and staging. Osteoarthritis Cartilage 14: 1-2, 2006.
27. Haseeb A and Haqqi TM: Immunopathogenesis of osteoarthritis. Clin Immunol 146: 185-196, 2013.
28. Chang X, Kang Y, Yang Y, Chen Y, Shen Y, Jiang C and Shen Y: Pyroptosis: A novel intervention target in the progression of osteoarthritis. J Inflamm Res 15: 3859-3871, 2022.
29. Huang Z and Kraus VB: Does lipopolysaccharide-mediated inflammation have a role in OA?. Nat Rev Rheumatol 12: 123-129, 2016.
30. Tall AR and Westerterp M: Inflammasomes, neutrophil extracellular traps, and cholesterol. J Lipid Res 60: 721-727, 2019.
31. Zhang Y, Lin Z, Chen D and He Y: CY-09 attenuates the progression of osteoarthritis via inhibiting NLRP3 inflammasome-mediated pyroptosis. Biochem Biophys Res Commun 553: 119-125, 2021.
32. Zhang L, Ma S, Su H and Cheng J: Isoliquiritigenin Inhibits IL-1β-Induced production of matrix metalloproteinase in articular chondrocytes. Mol Ther Methods Clin Dev 9: 153-159, 2018.
33. Bai L, Gao J, Wei F, Zhao J, Wang D and Wei J: Therapeutic potential of ginsenosides as an adjuvant treatment for diabetes. Front Pharmacol 9: 423, 2018.
34. Ding L, Gu S, Zhou B, Wang M, Zhang Y, Wu S, Zou H, Zhao G, Gao Z and Xu L: Ginsenoside compound K enhances fracture healing via promoting osteogenesis and angiogenesis. Front Pharmacol 13: 855393, 2022.